Available online at www.sciencedirect.com
ScienceDirect
Polymer 48 (2007) 2649–2658
polymer
www.elsevier.com/locate/polymer

Impacts of stereoregularity and stereocomplex formation on physicochemical, protein adsorption and cell adhesion behaviors of star-shaped 8-arms poly(ethylene glycol)–poly(lactide) block copolymer films

Koji Nagahama, Yoshihiro Nishimura, Yuichi Ohya*, Tatsuro Ouchi*

Department of Applied Chemistry, Faculty of Engineering and High Technology Research Center, Kansai University, Suita, Osaka 564-8680, Japan

Received 12 January 2007; received in revised form 2 March 2007; accepted 7 March 2007
Available online 12 March 2007

Abstract

Biodegradable stereocomplex film exhibiting soft and stretchy character was prepared by simply blending between enantiomeric 8-arms poly(ethylene glycol)-*block*-poly(L-lactide) (8-arms PEG-*b*-PLLA) and 8-arms PEG-*b*-PDLA copolymers with star-shaped structure. The stereocomplex film exhibited higher T_g and PLA crystallinity than those of original copolymer films. Effects of stereoregularity and stereocomplexation on protein adsorption and L929 cells attachment/proliferation behaviors onto the films were analyzed from the viewpoint to design a new class of implantable soft biomaterial. The stereocomplex film was found to exhibit large amount of protein adsorption than original films. Furthermore, cell attachment efficiency and proliferation rate on the film were significantly enhanced by stereocomplexation. This stereocomplex material is expected to be applicable as degradable temporary scaffold for soft tissue regeneration. Consequently, it was indicated that the stereocomplex formation could be proposed to be a novel method to control the protein- and cell-adhesive properties of biodegradable matrix composed of PEG–PLA copolymer.

Keywords: Stereocomplex; Polylactide; 8-Arms poly(ethylene glycol)

1. Introduction

Among the biodegradable polymers thus developed, polylactides (PLAs) have been receiving a special interest not only as eco-plastic materials but also as biomedical materials such as carrier for drug-delivery systems and temporary scaffold for the regeneration of various tissues [1–7]. The PLA synthesized from the enantiomeric L- and D-lactic acids are poly(L-lactide) (PLLA) and poly(D-lactide) (PDLA), respectively. PLLA and PDLA similar to other chiral polymers can form a racemate, the physical properties of which are different from those of the individual enantiomers. The racemates of chiral polymers were called stereocomplexes although the formation of a racemate has nothing to do with complexation in its original sense. The stereocomplex of PLLA and PDLA was at first reported by Ikada et al. [8,9]. Later, these studies were expanded by several research groups to block and graft copolymers containing PLLA or PDLA as hydrophobic segments. Biodegradable hydrogels based on stereocomplex formation of PLLA and PDLA in water-soluble amphiphilic copolymers have attracted much attention in recent years for possible biomedical and pharmaceutical applications. These new types of hydorgels created in water through physical cross-linking are expected to show advantageous characteristics for the controlled release of pharmaceutical proteins [10–15].

On the other hand, it is also possible to create the stereocomplex matrices between water-insoluble polymers by

* Corresponding authors. Tel.: +81 6 6368 0818; fax: +81 6 6339 4026.
E-mail addresses: yohya@ipcku.kansai-u.ac.jp (Y. Ohya), touchi@ipcku.kansai-u.ac.jp (T. Ouchi).

0032-3861/$ - see front matter © 2007 Elsevier Ltd. All rights reserved.
doi:10.1016/j.polymer.2007.03.017

a solvent-precipitation, layer-by-layer assembly or casting method [16–18]. A stereocomplex crystallite having a 3/1 helical structure is different from a homopolymer crystallite with a 10/3 helical structure found in individual PLLA or PDLA. More compact side-by-side crystallization between the two enantiomeric polymers results in a much higher melting point than that of homopolymer [19]. Biodegradable copolymers having higher mechanical strength, improved thermal stability, and a more hydrolysis-resistant property by simply blending amphiphilic copolymers consisting PLLA and PDLA are significant for development of a new class of implantable biomedical materials [20]. On the other hand, protein- and cell-adhesive properties on the surfaces of the amphiphilic copolymeric materials are important when the materials initially make contact with bio-systems. Therefore, it is essential to analyze the influences of stereoregularity of PLLA and PDLA and the stereocomplex formation on protein- and cell-adhesive properties of amphiphilic copolymer materials containing PLLA or PDLA for determining the potential for biomedical applications. However, to the best of our knowledge, such researches have not been reported so far.

Various amphiphilic block copolymers composed of PLLA and poly(ethylene glycol) (PEG) have been synthesized to attain versatile biodegradable polymers [21–26]. In our previous study, we synthesized star-shaped 8-arms poly(ethylene glycol)–poly(L-lactide) block copolymer (8-arms PEG-*b*-PLLA) and discussed the physicochemical properties as well as protein adsorption and cell attachment behaviors of its solution cast film [27,28].

In this article, water-insoluble two biodegradable star-shaped block copolymers of 8-arms PEG-*b*-PLLA and 8-arms PEG-*b*-PDLA with same chemical component but different stereoregularity were synthesized. By simply blending the star-shaped 8-arms PEG-*b*-PLLA and 8-arms PEG-*b*-PDLA with having no PLA crystallite, we prepared stereocomplex film with transparency. The stereocomplex formation was confirmed by differential scanning calorimetry (DSC) and wide-angle X-ray diffraction measurements. Physicochemical properties such as thermal, mechanical, surface and degradation of copolymer films were compared among the original copolymer and stereocomplex films. Additionally, we analyzed adsorption of plasma proteins and attachment/proliferation of L929 mouse fibroblast cells on the stereocomplex copolymer film and original copolymer films with different stereoregularity from the viewpoint to design a new class of implantable soft biomaterial.

2. Materials and methods

2.1. Materials

L-Lactide and D-lactide were purchased from PURAC. 8-Arms PEG ($M_n = 2.0 \times 10^4$, $M_w/M_n = 1.2$) was supplied by NOF Co. L-Lactide, D-lactide and 8-arms PEG were sufficiently dried under vacuum prior to use. Dry THF purchased from Wako Pure Chemical was used as a polymerization solvent. Other organic solvents were used without further purification. Plasma proteins such as bovine serum albumin and bovine plasma fibrinogen were purchased from Sigma Co. Ltd. and were used without further purification. Mouse fibroblast NCTC clone 929 (L929, lot# IFO50409) cells were supplied from the Health Science Research Resources Bank (HSRRB, Japan). Eagle's minimum essential medium (E-MEM) was purchased from Nissui Pharmaceutical.

2.2. Synthesis of copolymer and preparation of solution cast films

Star-shaped enantiomeric 8-arms PEG-*b*-PLLA and 8-arms PEG-*b*-PDLA copolymers were synthesized by ring-opening anionic polymerization of L-lactide and D-lactide using 8-arms PEG as an octafunctional macroinitiator (Scheme 1) [27]. The purification of the reaction products was performed three times by reprecipitation method using chloroform as a solvent and diethyl ether as a non-solvent, and dried under vacuum overnight to obtain the white solid 8-arms PEG-*b*-PLLA and 8-arms PEG-*b*-PDLA. The degree of polymerization of LLA and DLA, and the composition of the obtained block copolymers were determined by ^{1}H NMR (JEOL GSX-400, $CDCl_3$). The number-averaged molecular weight (M_n) and the molecular weight distribution (M_w/M_n) of the block copolymers were estimated by gel permeation chromatography [GPC; Tosoh GPC-8020 series system (column: TSK-GEL ALPHA-5000 × 2, eluent: DMF, detector: refractive index, standard: PEG)]. The stereocomplex (SC) film used for subsequent measurements was prepared by solution cast method. The acetonitrile solution of 8-arms PEG-*b*-PLLA and 8-arms PEG-*b*-PDLA was separately prepared to

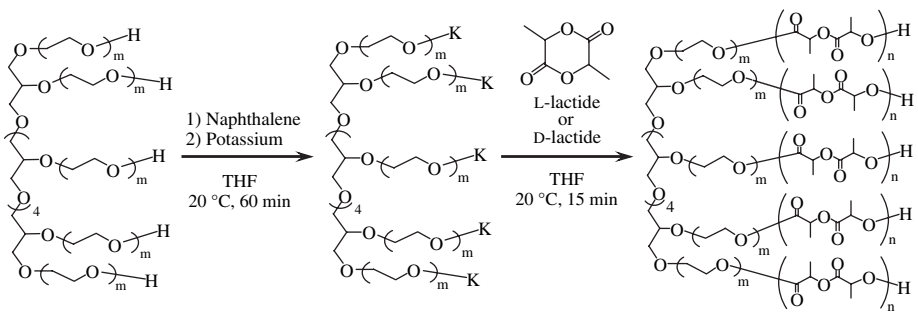

Scheme 1. Synthesis of 8-arms PEG-*b*-PL(D)LA copolymers.

have a polymer concentration of 50 mg/ml and then admixed with each other (the mixing ratio was fixed to 1:1) under vigorously stirring at 60 °C for 12 h. The mixed solution was cast onto Teflon dish (diameter: 70 mm), followed by solvent evaporation at room temperature for 2 days, and further dried thoroughly under vacuum for 7 days. As the control, the cast films of linear PLLA, PDLA and PLLA/PDLA SC films were prepared using the same procedure described above. The thickness of the polymer films and the SC films was in the range 100–120 μm.

2.3. Measurements of physicochemical properties of the polymer films

T_g, T_m, ΔH_m of the polymer films were measured by differential scanning calorimetry (DSC; SHIMADZU DSC-60, TA-60WS). Polymer films (5 mg) were quenched with liquid nitrogen, and then first heating run and second heating run were conducted. The temperature range was between −100 °C and 250 °C at a heating rate of 10 °C/min. Wide-angle X-ray diffraction analysis of the obtained polymer films was performed using M18XHF22-SRA (MAC Science Co.) with Cu Kα source ($\lambda = 1.54$ Å) at 25 °C. Tensile tests were performed using dry cast film by AUTOGRAPH AGS-J series equipment (SHIMAZU) at 25 °C. Test samples of the polymer film (dumbbell-shaped; both ends: 5 mm, middle: 2 mm, length: 40 mm) were prepared and subjected to the tensile test at an extension rate of 10 mm/min. Ten samples were tested and the results were averaged.

2.4. Measurement of water absorption and water contact angle of the polymer films

Water absorption of the copolymer films was examined by gravimetric measurement. The copolymer films were weighed and immersed in a 1/15 M KH_2PO_4–$NaHPO_4$ buffer (PBS; pH = 7.4, $I = 0.14$) at 37 °C. At preset time intervals, the films were taken out and interposed between pieces of wet filter paper to remove water droplets from the film surfaces. The water absorption of the films was evaluated based on the weight increase. Water absorption of polymer films was determined as follows: water absorption $(\%) = [(W_{wet} - W_{dry})/W_{dry}] \times 100$. Dynamic contact angles of the air side of the block copolymer films against water were measured by the sessile drop method at 25 °C with the help of a CCD camera to evaluate the wettabilities of film surfaces. The average values were determined from measurements at 15 different points on the films excluding the maximum and minimum values.

2.5. Protein adsorption behavior

Protein adsorption onto copolymer film surfaces was measured using albumin/PBS(−) and fibrinogen/PBS(−) solutions at concentrations of 45 mg/ml and 3.0 mg/ml, respectively. Each copolymer was dissolved in chloroform (4 wt%) and then cast on a glass dish (diameter: 30 mm) to form a film. The obtained film was then dried in air for 2 days, and then further dried under vacuum for 4 days. Prior to the protein adsorption experiment, the copolymer films were exposed to PBS(−) at 37 °C for 60 min to obtain equilibrium water absorption films. The block copolymer films were then placed in 2 ml of protein solution at 37 °C for 2 h, followed by double dilution displacement rinsing with PBS(−). To elute the adsorbed protein from the film surfaces, the block copolymer films were vigorously washed several times with a 2% (w/v) PBS(−) solution containing sodium dodecyl sulfate (SDS). A protein analysis kit (micro BCA protein assay regent kit, Pierce) based on the bicinchoninic acid (BCA) method was used to determine the concentration of the protein in the SDS solution [29,30].

2.6. Cell culture

Mouse fibroblast L929 cells were subcultured in E-MEM supplemented with 10% (v/v) fetal calf serum (FCS, JRH Bioscience) and harvested with PBS(−) (Nissui Pharmaceutical) containing 0.025% (w/v) trypsin and 0.01% ethylenediaminetetraacetic acid. The medium was changed every 3 days.

2.7. Cell attachment and proliferation test

Each copolymer was dissolved in chloroform (4 wt%) and then cast on a glass dish (diameter: 30 mm) to form a film. The polymer films were used after being sterilized with UV irradiation for 1 h. A suspension of mouse fibroblast L929 cells (2.0 ml, 1.25×10^5 cells/ml) in E-MEM containing 10% (v/v) fetal calf serum (FCS, JRH Bioscience) was distributed onto polymer films in the glass dishes followed by culturing in a humidified atmosphere containing 5% CO_2 at 37 °C. After incubation, the films were rinsed 3 times with E-MEM to remove non-attached cells. The number of cells attached to the film surfaces was measured using an MTT assay. E-MEM (2.19 ml) and an aqueous MTT solution (438 μl) were added to the films followed by incubation at 37 °C for 4 h. The resulting formazan precipitate was then dissolved by the addition of a 0.04 M HCl/*iso*-propanol solution (2.19 ml) containing 10% Triton X-100. Aliquots of the supernatant of the solution in the dishes were then transferred into 96-well microplates. The absorbance of this solution at 630 nm was measured using a microplate reader (MTP-120, Corona Electric). The number of cells attached was expressed as a percentage of the initial cell number (2.5×10^5 cells). Cell proliferation was investigated after 1–14 days. The number of cells after incubation was measured by the same methods as described above, where the initial number of cells was adjusted to 5.0×10^4 cells/dish. The medium was exchanged every 3 days. To evaluate the morphology of adherent cells on the surface of the polymer films after 14 days, phase contrast images were taken.

2.8. Film degradation test

The biodegradation behavior of polymer films was estimated by weight loss. The polymer films (10 mm × 20 mm) were weighted after thorough drying (W_0) and immersed in

PBS (pH = 7.4, $I = 0.14$) at 37 °C. After 4, 7, 14, 21 and 28 days, the polymer films were taken out from PBS, washed with water, dried in vacuo, and then weighted again (W_t). The weight loss was determined as follows: weight loss (%) = $[(W_0 - W_t)/W_0] \times 100$.

3. Results and discussion

3.1. Characterization of polymer films

The molecular characteristics and thermal properties of polymer films utilized in this study are listed in Table 1. We use code name such as 8-arms PEG20K-*b*-PLLA50K, where 20 K means the molecular weight of 8-arms PEG unit is 20,000 and 50 K means the total molecular weight of PLLA segments is 50,000, respectively. We successfully synthesized enantiomeric star-shaped copolymers having same compositions of PEG and PL(D)LA to make form the stereocomplex. T_g of original 8-arms PEG20K-*b*-PLLA50K and 8-arms PEG20K-*b*-PDLA46K films were drastically lower than those of PLLA53K and PDLA50K films. On the other hand, T_g of mixed film between 8-arms PEG20K-*b*-PLLA50K and 8-arms PEG20K-*b*-PDLA46K was higher than that of original copolymer films. No endothermal peaks were detected in the DSC curves of both 8-arms PEG20K-*b*-PLLA50K and the 8-arms PEG20K-*b*-PDLA46K films. On the contrary, the mixed film clearly showed only one endothermal peak at 194 °C assigned to the T_m of PLA crystallites. Namely the equimolar mixed film had no PEG crystallite. So, the crystallinity (X_c) of PLA in the mixed film was determined as follows: X_c (%) = $(\Delta H_m/\Delta H_{m,\ 100\%}) \times 100$, where ΔH_m was the melting enthalpy of PLA in the mixed films, $\Delta H_{m,\ 100\%}$ was the melting enthalpy of perfect PLA crystallites (−93.7 J/g). Although X_c of PLA for both 8-arms PEG20K-*b*-PLLA50K and the 8-arms PEG20K-*b*-PDLA46K films was 0.0%, that of equimolar mixed film was 17.5%. Therefore, the crystalline structure of each copolymer film was analyzed by wide-angle X-ray diffraction measurement (WAXD). Fig. 1 shows the WAXD spectra of original 8-arms PEG20K-*b*-PLLA50K and 8-arms PEG20K-*b*-PDLA46K films as well as the mixed film. It

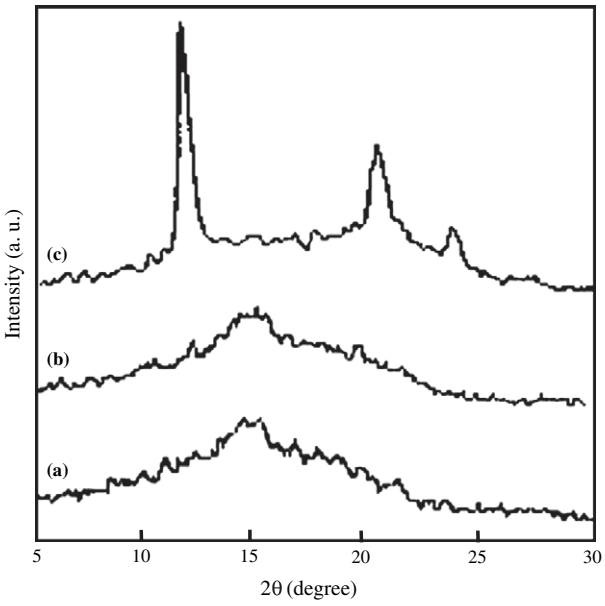

Fig. 1. Wide-angle X-ray diffraction patterns of (a) 8-arms PEG20K-*b*-PLLA50K film, (b) 8-arms PEG20K-*b*-PDLA47K film, and (c) their 50/50 mixed film.

was well known that the diffraction peaks of homo-PLLA and PDLA crystallite appeared at $2\theta = 16.8°$, 19.1°, and 22.5° [8]. In addition, the two peaks of PEG crystallite were detected at $2\theta = 19.4°$ and 23.6°. However, no crystalline peaks were detected in the WAXD patterns of both 8-arms PEG20K-*b*-PLLA50K and the 8-arms PEG20K-*b*-PDLA46K films. This result indicates that the formation of the PLA as well as PEG crystallites was strongly suppressed by introduction of star-shaped structure. Thus, it was revealed that the original 8-arms PEG20K-*b*-PLLA50K and 8-arms PEG20K-*b*-PDLA46K films exhibited amorphous states. On the contrary, the mixed film clearly showed three diffraction peaks at $2\theta = 12.0°$, 21.6°, and 23.8°. These peaks were reasonably assigned to the stereocomplex crystallites comprised of PLLA and PDLA. Therefore, it was confirmed that the amorphous 8-arms PEG20K-*b*-PLLA50K and the 8-arms PEG20K-*b*-PDLA47K were able to form the stereocomplex crystallites.

Table 1
Characteristics of 8-arms PEG, copolymer and PL(D)LA films used in this study

Polymer	M_n[a] × 10^{-4} (M_w/M_n)[a]	[*m*,*n*][b]	T_g[c] (°C)	T_m[c] (°C)		X_c of PL(D)LA[d] (%)
				PEG	PL(D)LA	
8-Arms PEG20K	2.0 (1.08)	[57,−]	−10.3	50.6	−	−
8-Arms PEG20K-*b*-PLLA50K	6.9 (1.32)	[57,43]	−9.5	N.D.[e]	N.D.[e]	0.0
8-Arms PEG20K-*b*-PDLA46K	6.7 (1.25)	[57,41]	−11.7	N.D.[e]	N.D.[e]	0.0
SC (block copolymer)	−	−	3.6	N.D.[e]	194.0	17.5
PLLA53K	5.3 (1.35)	[−,367]	56.2	−	173.9	47.3
PDLA50K	5.0 (1.31)	[−,347]	53.7	−	172.6	46.8

[a] Estimated by GPC (eluent: DMF, standard: PEG).
[b] [*m*,*n*]: Degree of polymerization of ethylene glycol unit and L- (or D-) lactide unit, respectively. *m* and *n* values were estimated by ^{1}H NMR spectroscopy (solvent: $CDCl_3$).
[c] Determined by DSC. The film (6 mg) was heated at 10 °C/min.
[d] Crystallinity (X_c) estimated from ΔH value obtained by DSC measurement.
[e] Not detected.

Since a diffraction peak except the stereocomplex crystallites was not detected in the mixed film, it was estimated that the stereocomplex crystallites were dispersed into continuous amorphous PEG phase within the film.

3.2. Wettability of the polymer film

Investigating the interaction between water and any material to be used as a biological implant is very important. So, we evaluated the water absorption capacity of the copolymer films. The time-course curves of water absorption of polymer films in PBS are shown in Fig. 2. In both original 8-arms PEG20K-*b*-PLLA50K and 8-arms PEG20K-*b*-PDLA46K films, water absorption started immediately after immersion in PBS and then leveled off after 60 min (equilibrium water absorption). In comparison, the stereocomplex film exhibited a much slower water absorption rate, and did not level off after 240 min. This directly implies that the higher crystallinity of the stereocomplex film, which made the internal polymer structure inaccessible to water, resulted in a slow hydration rate of the PEG chains in the stereocomplex films.

The water dynamic contact angles of the polymer film surfaces were compared to evaluate the surface wettability of these films. The surface contact angles of the block copolymer films are shown in Table 2. The values of the water contact angles of 8-arms PEG20K-*b*-PLLA50K, 8-arms PEG20K-*b*-PDLA46K and stereocomplex films were found to be 52.4°, 50.8° and 64.8°, respectively. Although the hydrophilic PEG contents were the same among the three copolymer films, water contact angle of the stereocomplex film surface was significantly higher than that of the original copolymer films. The difference in contact angle may be related to many factors,

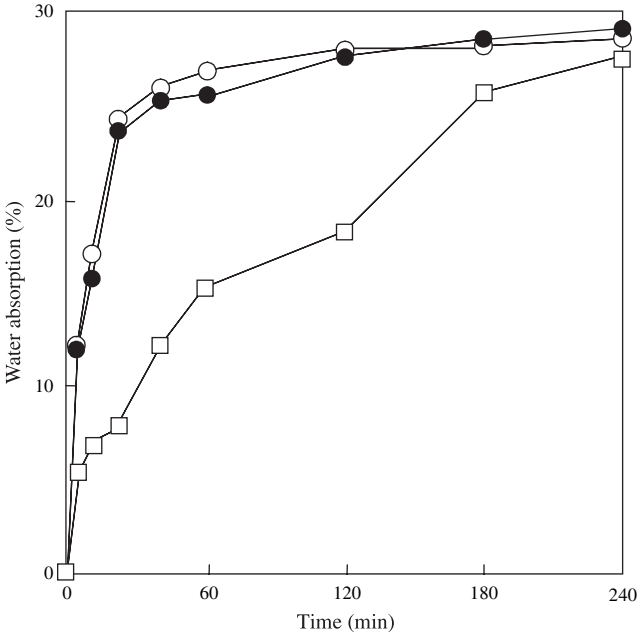

Fig. 2. The water absorption of (○) 8-arms PEG20K-*b*-PLLA50K film, (●) 8-arms PEG20K-*b*-PDLA46K film, and (□) SC film in PBS (pH = 7.4, $I = 0.14$) at 37 °C as a function of time.

Table 2
Dynamic contact angles against water of copolymer films

Copolymer	Contact angles (°)		
	Advancing (θ_a)	Receding (θ_r)	Hysteresis (θ)
8-Arms PEG20K-*b*-PLLA50K	66.5	38.3	28.2
8-Arms PEG20K-*b*-PDLA46K	64.8	36.8	28.0
SC (block copolymer)	81.7	51.7	30.0

including surface roughness, patch-wise heterogeneity, deformation, liquid penetration, swelling, and the mobility of chains. The large difference in contact angle among PEG–PLA copolymer films may be mainly attributed to the degree of mobility of the PEG chains located near the surface of the material. Practically, it was confirmed by SEM observation that the surfaces of the prepared films were flat and that the films had no porous structure in the bulk phase (data not shown). It is suggested that the influence of the surface roughness on the dynamic contact angles and water absorption measurements, cell attachment, and growth can be ignored. These results suggest that the migration of the PEG chains from inside to surface of the stereocomplex film was suppressed by stereocomplex crystallites dispersed into continuous amorphous PEG phase within the film. Considering these results, it was expected that the surface wettability of PEG–PLA block copolymer film was controllable by adjusting the degree of stereocomplex crystallinity.

3.3. Protein adsorption onto copolymer films

Plasma protein adsorption is one of the most important phenomena in determination of the biocompatibility of the implantable materials [31,32]. The equilibrium amounts of plasma proteins such as bovine serum albumin (BSA) and bovine plasma fibrinogen adsorbed onto the original copolymer and stereocomplex film surfaces with different stereoregularity are shown in Fig. 3. The amounts of BSA and fibrinogen that adsorbed onto original 8-arms PEG20K-*b*-PLLA50K and 8-arms PEG20K-*b*-PDLA46K films were almost the same level. This indicated that the amounts of the plasma protein adsorption were independent on the stereoregularity of PLA. However, the amounts of the plasma protein adsorption onto the stereocomplex film were effectively higher than that onto the original films. The results are consistent with the results for the dynamic water contact angles of copolymer films. Accordingly, it was suggested that the increase in the plasma protein adsorption onto the stereocomplex film was attributed to the low density of the PEG chains located near the film surface. It was suggested that the rapid migration of many PEG chains from the interior to the surface in the homogeneous 8-arms PEG20K-*b*-PLLA50K and 8-arms PEG20K-*b*-PDLA46K films with amorphous state suppresses plasma protein (BSA and fibrinogen) adsorption effectively. On the contrary, stereocomplex crystallites located near the surface area of the film promoted the plasma protein adsorption. A large increase of the plasma protein adsorption on stereocomplex film is very significant for cell attachment and proliferation from the

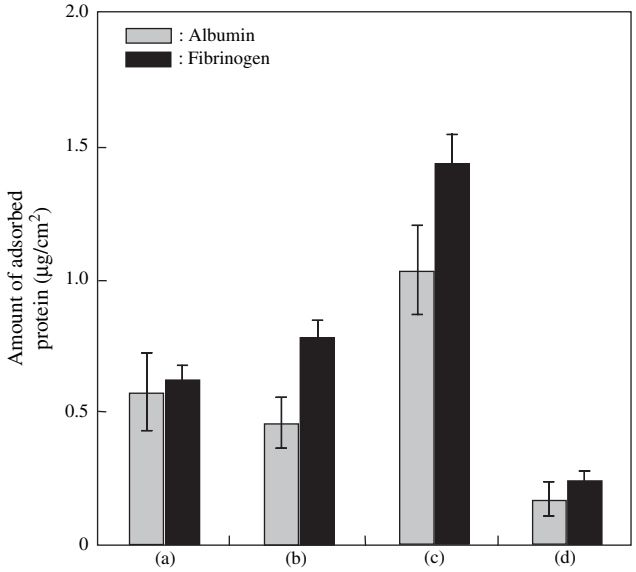

Fig. 3. Amount of plasma proteins adsorbed onto (a) 8-arms PEG20K-*b*-PLLA50K film, (b) 8-arms PEG20K-*b*-PDLA46K film, (c) SC film, and (d) glass surfaces after incubation at 37 °C for 2 h.

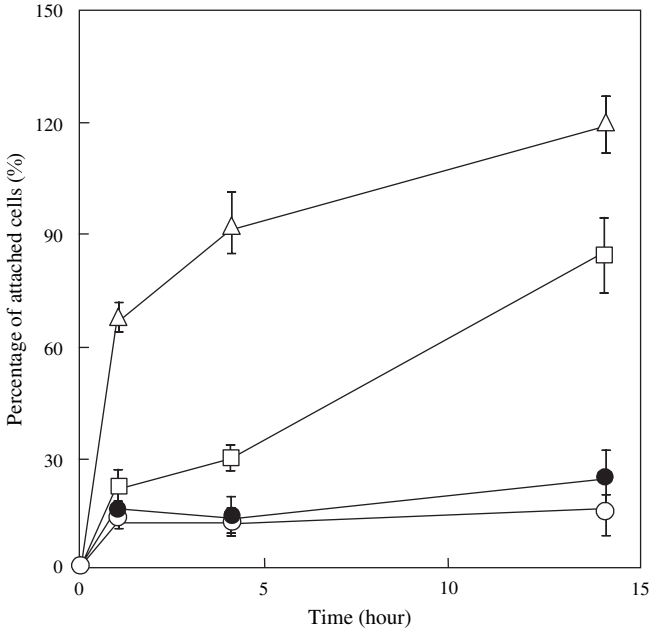

Fig. 4. The percentage of L929 cells attached onto (○) 8-arms PEG20K-*b*-PLLA50K film, (●) 8-arms PEG20K-*b*-PDLA46K film, (□) SC film, and (△) TCPS surfaces.

standpoint of utilizing as temporary scaffolds to support tissue regeneration.

3.4. Cell attachment behavior onto copolymer films

In the present study, PLA with different stereoregularity and the same chemical components were used. Accordingly, the effects of the stereoregularity of PLA on L929 fibroblast cell attachment and proliferation were investigated by using the original 8-arms PEG20K-*b*-PLLA50K and 8-arms PEG20K-*b*-PDLA46K films as well as the stereocomplex film. Fig. 4 shows the percentages of L929 cells that attached to each film compared to the number of cells that attached to tissue culture polystyrene (TCPS) as a control after 1–14 h of incubation in a medium containing serum. The number of L929 cells attached to any of the films increased with incubation time. For the initial 4 h, the stereocomplex film composed of 8-arms PEG20K-*b*-PLLA50K and 8-arms PEG20K-*b*-PDLA46K with different stereoregularity exhibited somewhat higher L929 cell attachment than the original copolymer films. After 14 h of incubation, the L929 cell attachment efficiency of stereocomplex film was drastically higher than that of original copolymer films. Thus, it was suggested that L929 cell attachment efficiency was significantly enhanced by stereocomplex formation. From these results, it was found that efficient attachment of L929 cells onto the film surface was independent of the stereoregularity of PLAs in the 8-arms PEG20K-*b*-PLLA50K and 8-arms PEG20K-*b*-PDLA46K films. On the other hand, it was revealed that stereocomplex formation between 8-arms PEG20K-*b*-PLLA50K and 8-arms PEG20K-*b*-PDLA46K influenced the L929 cell attachment onto the film surface. The wettability and the amount of the plasma protein adsorption of the films are well known key factors that affect cell attachment. The results from surface contact angle and plasma protein adsorption (BSA and fibrinogen) of the films strongly supported the results in L929 cell attachment for stereocomplex film. Namely, it was concluded that the appropriate wettability as well as the large amount of plasma protein adsorption led to the high L929 cell attachment efficiency in the stereocomplex film.

3.5. Cell proliferation behavior onto copolymer films

Cell proliferation was analyzed by the incubation of L929 cells for 14 days onto each film, as shown in Fig. 5. The tendency observed in this case was almost similar to the results obtained for cell attachment. The stereocomplex film gave the highest L929 cell growth ability among the copolymer films tested for 14 days. Significant differences in the number of adherent L929 cells were not observed until 4 days. However, after 7 days, the difference in growth rate was apparent among copolymer films. The number of L929 cells on two original copolymer films after 14 days of incubation was about 60% of that onto the stereocomplex film. These observations indicated that the stereocomplex formation mainly affected the proliferation of L929 cells at the late stages.

In order to evaluate the cell proliferation behavior in detail, the adherent cells after 4 days were observed directly by phase contrast microscopy, as shown in Fig. 6. The L929 cells onto both TCPS and stereocomplex film exhibited the adequate shape for continual cell proliferation, while the L929 cells onto the original copolymer films exhibited the flattened shape. These results are consistent with the number of adherent L929 cells estimated by MTT assay. Consequently, it was indicated that the stereocomplex formation could be proposed to be a novel method to control not only the flexibility but also plasma protein- and L929 cell-adhesive properties of biodegradable matrix composed of PEG–PLA copolymer.

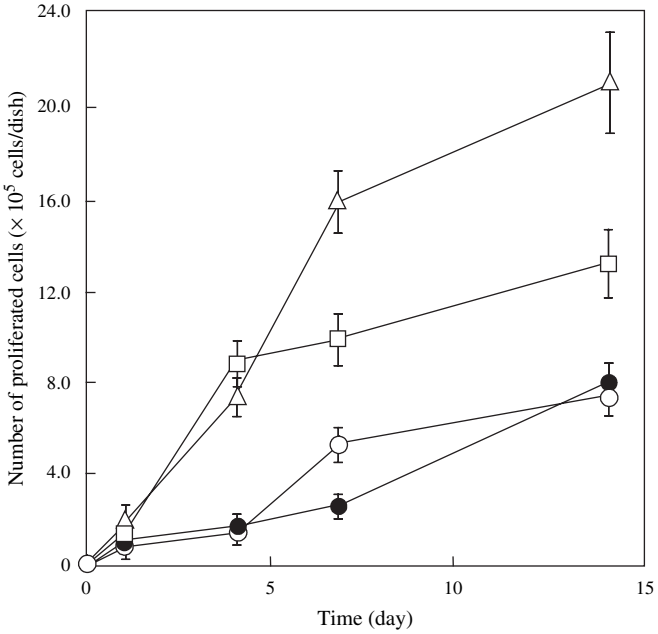

Fig. 5. Number of L929 cells proliferated onto (○) 8-arms PEG20K-*b*-PLLA50K film, (●) 8-arms PEG20K-*b*-PDLA46K film, (□) SC film, and (△) TCPS surfaces.

3.6. Tensile property of polymer films

The tensile properties of dry copolymer films and equilibrium water absorption copolymer films were evaluated from their stress–strain curves, as shown in Fig. 7A and B. 8-Arms PEG20K-*b*-PLLA50K and 8-arms PEG20K-*b*-PDLA dry films showed lower tensile strength and higher elongation at break than those of the PLLA53K and PDLA50K films. So, these tensile profiles mean the softness of 8-arms PEG20K-*b*-PLLA50K and 8-arms PEG20K-*b*-PDLA46K dry films. The dry stereocomplex film between PLLA53K and PDLA50K showed equivalent fracture elongation (18%) and quite higher tensile strength (57 MPa) compared with those of dry original copolymer films. However, it was quite interesting that the dry stereocomplex film between 8-arms PEG20K-*b*-PLLA50K and 8-arms PEG20K-*b*-PDLA46K showed the equivalent tensile strength (12 MPa) and the effectively higher fracture elongation (165%) compared with those of dry original copolymer films. Fig. 7B shows stress–strain curves of equilibrium water absorption copolymer films. The equilibrium water absorption copolymer films exhibited similar tendency as dry copolymer films, while the elongation at break slightly decreased.

Consequently, stereocomplex formation between enantiomeric PLLA and PDLA chains in amorphous states gave the softness as well as tenacity to stereocomplex film composed of 8-arms PEG20K-*b*-PLLA50K and 8-arms PEG20K-*b*-PDLA46K. It was indicated that the appropriately dispersed stereocomplex crystallite domains into continuous amorphous PEG phase played a key role in its mechanical property. The easy stereocomplex formation between PLLA and PDLA chains bearing at the ends of star-shaped 8-arms PEG chains afforded the physical PEG network; the stereocomplex crystallite domains were expected to act as physical cross-linking points within continuous amorphous PEG phase, so that the stereocomplex films composed of 8-arms PEG20K-*b*-PLLA50K and 8-arms PEG20K-*b*-PDLA46K showed the

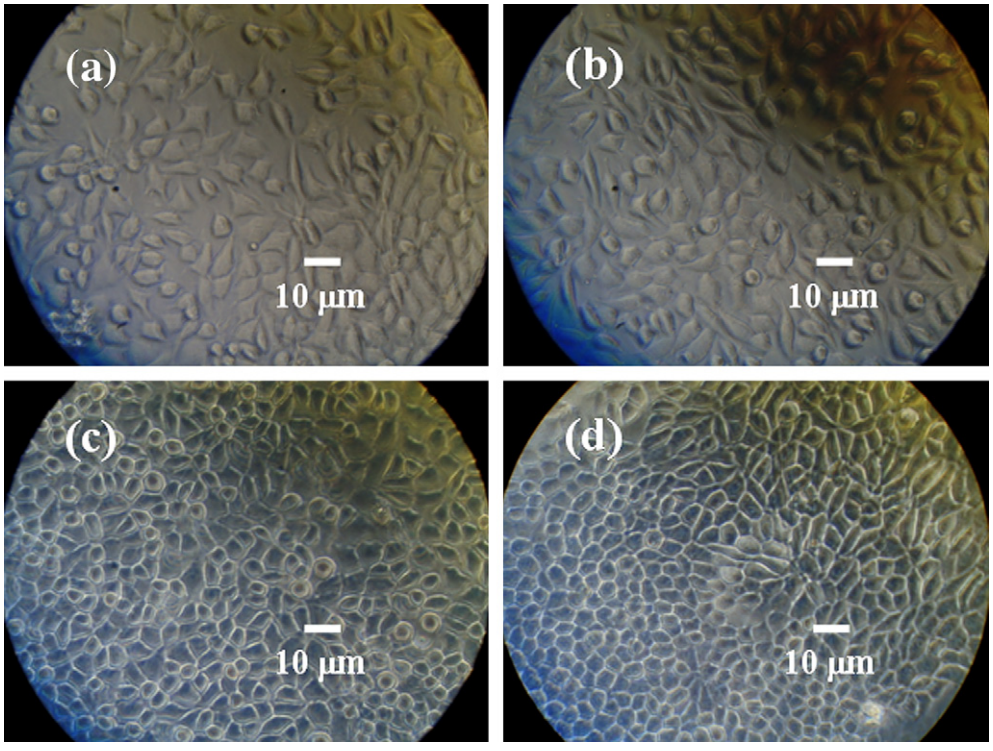

Fig. 6. Phase contrast images of L929 cells adhering onto (a) 8-arms PEG20K-*b*-PLLA50K film, (b) 8-arms PEG20K-*b*-PDLA46K film, (c) SC film, and (d) TCPS surfaces at 4 days after cell seeding.

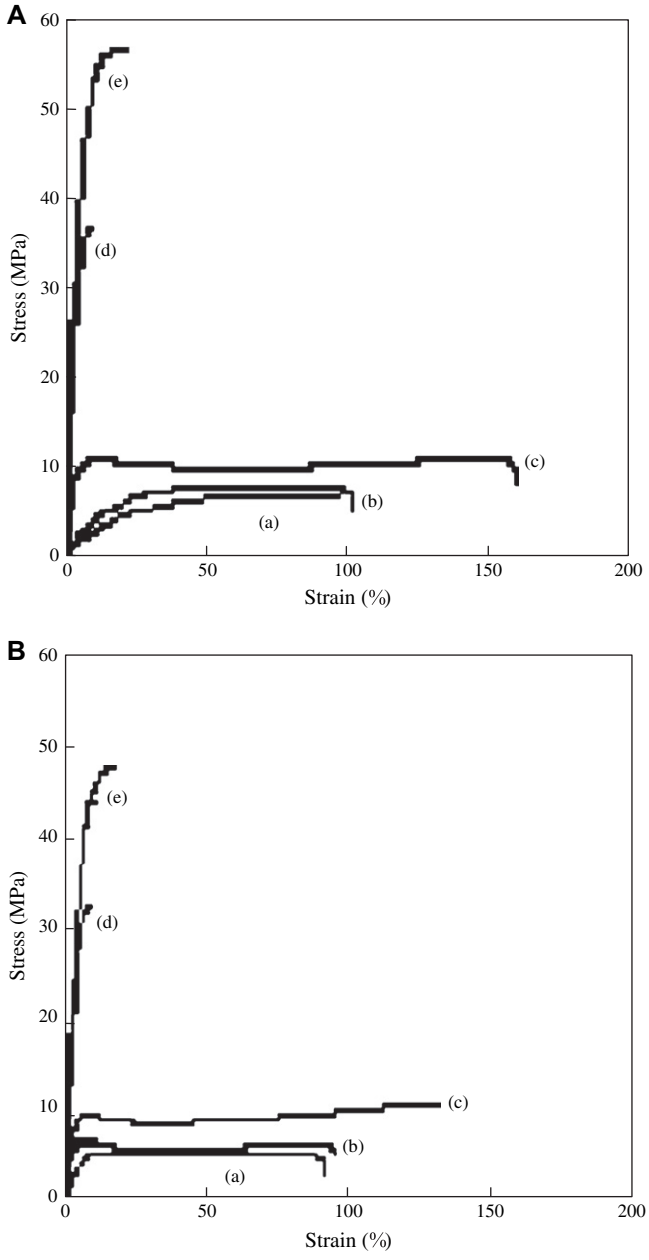

Fig. 7. Stress–strain curves of (a) 8-arms PEG20K-*b*-PLLA50K film, (b) 8-arms PEG20K-*b*-PDLA46K film, (c) SC film, (d) PLLA53K film, and (e) PLLA53K/PDLA50K SC film. (A) As cast dry film and (B) equilibrium water absorption film.

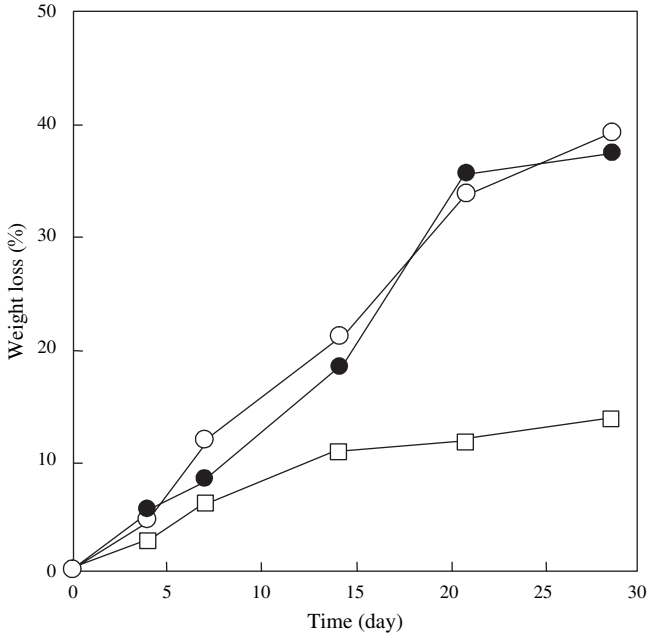

Fig. 8. Time courses of weight reduction of (○) 8-arms PEG20K-*b*-PLLA50K film, (●) 8-arms PEG20K-*b*-PDLA46K film, and (□) SC film in PBS (pH = 7.4, $I = 0.14$) at 37 °C.

good mechanical properties as implantable soft biomaterials contacting with tissues and organs.

3.7. Film degradation behavior

The degradation behavior of copolymer films with different stereoregularity was evaluated in vitro. Fig. 8 shows the time-course curves of the weight loss (%) of copolymer films during the biodegradation test in PBS at 37 °C. The similar rates of weight loss were observed in original 8-arms PEG20K-*b*-PLLA50K and 8-arms PEG20K-*b*-PDLA46K films. This indicated that the degradation behavior was independent of the stereoregularity of PLA. However, stereocomplex film exhibited the lowest degradation rate among the copolymer films tested for 28 days. Similar tendency in the weight loss was observed among the copolymer films until 7 days. On the contrary, after 7 days, significant differences in degradation rates were apparent among copolymer films. The weight loss of two original copolymer films after 28 days of incubation was about 310% of that the stereocomplex film. These observation results indicated that the stereocomplex formation mainly affected the film degradation at the late stages. The stereocomplex formation led to an increase of crystallinity. So, the decrease of the volume fraction of noncrystalline region suppressed the diffusion of water molecule and subsequently lowered the hydrolytic degradation rate. These results suggested that the control of matrix degradability may be possible by varying the degree of stereocomplex formation using different mixing ratio of enantiomeric 8-arms PEG20K-*b*-PLLA50K and 8-arms PEG20K-*b*-PDLA46K copolymers.

4. Conclusion

Biodegradable stereocomplex film composed of enantiomeric 8-arms PEG20K-*b*-PLLA50K and 8-arms PEG20K-*b*-PDLA46K copolymers was developed. In the present study, PLAs with different stereoregularity and the same chemical components were used. The effects of stereoregularity and stereocomplex formation on the physicochemical and surface properties of copolymer film as well as cell attachment and proliferation behavior of mouse fibroblast L929 cells onto copolymer films were investigated. We found that the stereocomplex film exhibited effectively higher surface contact

angle and larger amount of plasma protein (BSA and fibrinogen) adsorption than the original copolymer films. The L929 cell attachment efficiency and proliferation rate on stereocomplex film were effectively higher than those on the original copolymer films. Thus, it was concluded that L929 cell growth onto the film was significantly enhanced by stereocomplex formation. Furthermore, stereocomplex formation between enantiomeric PLLA and PDLA chains in amorphous PEG-PLA block copolymer gave the softness as well as tenacity to stereocomplex film composed of 8-arms PEG20K-*b*-PLLA50K and 8-arms PEG20K-*b*-PDLA46K copolymers. It was concluded that not only the stereoregularity of polymers but also the control of crystallinity is important in producing soft biomedical materials. Consequently, it was indicated that the stereocomplex formation could be proposed to be a novel method to control not only the flexibility but protein- and cell-adhesive properties of biodegradable matrix composed of PEG–PLA copolymer. Although it was difficult to adjust the minute crystallinity of PLA in the matrix, this stereocomplex matrix composed of 8-arms PEG-*b*-PL(D)LA copolymers is expected to be applicable as degradable temporary scaffold for tissue engineering.

Acknowledgements

The authors thank NOF Co. for the supply of 8-arms PEG. This work was financially supported by a Grant-in-Aid for Research (B) (17300163) from *The Japan Society for the Promotion of Science*. This work was carried out as a study in the High-Tech Research Center Project supported by *The Ministry of Education, Culture, Sports, Science and Technology, Japan*.

References

[1] Steinbuechel A. Biopolymers, vols. 3 and 4. Weinheim: Wiley-VCH; 2001.
[2] Tsuruta T, Hayashi K, Ishihara K, Kimura Y. Biomedical applications of polymeric materials. Boca Raton, FL: CRC Press; 1993.
[3] Frazza EJ, Schmitt EE. A new absorbable suture. J Biomed Mater Res Symp 1970;1:43–58.
[4] Ogawa Y, Yamamoto M, Ogawa H, Yashiki T, Shimamoto T. A new technique to efficiently entrap leuprolide acetate into microcapsules of polylactic acid or copoly(lactic/glycolic) acid. Chem Pharm Bull 1988;36:1095–103.
[5] Wise DL, Fellmann TD, Sanderson JE, Wentworth RL. Lactide/glycolic acid polymers. In: Gregoriadis GA, editor. Drug carriers in biology and medicine. London: Academic; 1979. p. 237–70.
[6] Echeverria EA, Jimenez J. Evaluation of an absorbable synthetic suture material. Surgery 1970;131:1–11.
[7] Vert M. Lactide polymerization faced with therapeutic application requirements. Macromol Symp 2000;153:333–42.
[8] Ikada Y, Jamshidi K, Tsuji H, Hyon SH. Stereocomplex formation between enantiomeric poly(lactides). Macromolecules 1987;20: 904–6.
[9] Tsuji H, Ikada Y. Blends of isotactic and atactic polylactides: 2. Molecular-weight effects of atactic component on crystallization and morphology of equimolar blends from the melt. Polymer 1996;37:595–602.
[10] De Jong SJ, De Smedt SC, Wahls MWC, Demeester J, Kettenesvan den Bosch JJ, Hennink WE. Novel self-assembled hydrogels by stereocomplex formation in aqueous solution of enantiomeric lactic acid oligomers grafted to dextran. Macromolecules 2000;33:3680–6.
[11] Lim DW, Choi SH, Park TG. A new class of biodegradable hydrogels stereocomplexed by enantiomeric oligo(lactide) side chains of poly-(HEMA-*g*-OLA)s. Macromol Rapid Commun 2000;21:464–71.
[12] Slivniak R, Domb AJ. Stereocomplexes of enantiomeric lactic acid and sebacic acid ester–anhydride triblock copolymers. Biomacromolecules 2002;3(4):754–60.
[13] Li SM, Vert M. Synthesis, characterization, and stereocomplex induced gelation of block copolymers prepared by ring-opening polymerization of L(D)-lactide in the presence of poly(ethylene glycol). Macromolecules 2003;36:8008–14.
[14] Mukose T, Fujiwara T, Nakano J, Taniguchi I, Miyamoto M, Kimura Y, et al. Hydrogel formation between enantiomeric B–A–B type block copolymers of polylactides (PLLA or PDLA: A) and polyoxyethylene (PEG: B); PEG–PLLA–PEG and PEG–PDLA–PEG. Macromol Biosci 2004;4:361–7.
[15] Hiemstra C, Zhong Z, Li L, Dijkstra PJ, Feijen J. In situ formation of biodegradable hydrogels by stereocomplexation of PEG–$(PLLA)_8$ and PEG–$(PDLA)_8$ star block copolymers. Biomacromolecules 2006;7: 2790–5.
[16] Serizawa T, Yamashita H, Fujiwara T, Kimura Y, Akashi M. Stepwise assembly of enantiomeric poly(lactide)s on surfaces. Macromolecules 2001;34:1996–2001.
[17] Lim DW, Park TG. Stereocomplex formation between enantiomeric PLA–PEG–PLA triblock copolymers: characterization and use as protein-delivery microparticulate carriers. J Appl Polym Sci 2000;75: 1615–23.
[18] Kricheldorf H, Rost S, Wutz C, Domb A. Stereocomplex of A–B–A triblock copolymers based on poly(L-lactide) and poly(D-lactide) A blocks. Macromolecules 2005;38:7018–25.
[19] Tsuji H, Ikada Y. Stereocomplex formation between enantiomeric poly-(lactic acids). 9. Stereocomplexation from the melt. Macromolecules 1993;26:6918–26.
[20] Li S, Vert M. Morphological changes resulting from the hydrolytic degradation of stereocopolymers derived from L- and DL-lactides. Macromolecules 1994;27:3107–10.
[21] Yamaoka T, Takahashi Y, Fujisato T, Lee CW, Tsuji T, Ohta T, et al. Novel adhesion prevention membrane based on a bioresorbable copoly(ester–ether) comprised of poly-L-lactide and pluronic: in vitro and in vivo evaluations. J Biomed Mater Res Part A 2000;54:470–9.
[22] Odelius K, Finne A, Albertsson AC. Versatile and controlled synthesis of resorbable star-shaped polymers using a spirocyclic tin initiator-reaction optimization and kinetics. J Polym Sci Part A Polym Chem 2005;44: 596–605.
[23] Breitenbach A, Li YX, Kissel T. Branched biodegradable polyesters for parenteral drug delivery systems. J Control Release 2000;64: 167–78.
[24] Dong Y, Feng S. Methoxy poly(ethylene glycol)–poly(lactide) (MPEG–PLA) nanoparticles for controlled delivery of anticancer drugs. Biomaterials 2004;25:2843–9.
[25] Lieb E, Tessmar J, Hacker M, Fischbach C, Rose D, Blunk T, et al. Poly (D,L-lactic acid)–poly(ethylene glycol)-monomethyl ether diblock copolymers control adhesion and osteoblastic differentiation of marrow stromal cells. Tissue Eng 2003;91:71–84.
[26] Otsuka H, Nagasaki Y, Kataoka K. Surface characterization of functionalized polylactide through the coating with heterobifunctional poly(ethylene glycol)/polylactide block copolymers. Biomacromolecules 2000;1: 39–48.
[27] Nagahama K, Ohya Y, Ouchi T. Synthesis of star-shaped 8 arms poly-(ethylene glycol)–poly(L-lactide) block copolymer and physicochemical properties of its solution cast film as soft biomaterial. Polym J 2006;38: 852–60.
[28] Nagahama K, Ohya Y, Ouchi T. The suppression of cell and platelet adhesion to star-shaped 8-arms poly(ethylene glycol)–poly(L-lactide) block copolymer films. Macromol Biosci 2006;6:412–9.

[29] Soltys-Robitaille CE, Ammon DM, Valint PL, Grobe GL. The relationship between contact lens surface charge and in-vitro protein deposition levels. Biomaterials 2001;22:3257–60.

[30] Gessner A, Lieske A, Paulke B, Mueller R. Influence of functional groups of polystyrene modified latex nanoparticles on protein adsorption. J Biomed Mater Res Part A 2003;65:319–26.

[31] Ishihara K, Ziats NP, Tierney BP, Nakabayashi N, Anderson JM. Protein adsorption from human plasma is reduced on phospholipid polymers. J Biomed Mater Res 1991;25:1397–407.

[32] Ishihara K, Oshida H, Endo Y, Ueda T, Watanabe A, Nakabayashi N. Hemocompatibility1of human whole blood on polymers with a phospholipid polar group and its mechanism. J Biomed Mater Res 1992;26:1543–52.